Liquid Crystals
Publication details, including instructions for authors and subscription information:
http://www.informaworld.com/smpp/title~content=t713926090

Computer simulation of a biaxial liquid crystal

Michael P. Allen[a]
[a] H. H. Wills Physics Laboratory, Bristol, England

To cite this Article Allen, Michael P.(1990) 'Computer simulation of a biaxial liquid crystal', Liquid Crystals, 8: 4, 499 — 511
To link to this Article: DOI: 10.1080/02678299008047365
URL: http://dx.doi.org/10.1080/02678299008047365

LIQUID CRYSTALS, 1990, VOL. 8, NO. 4, 499–511

Computer simulation of a biaxial liquid crystal

by MICHAEL P. ALLEN
H. H. Wills Physics Laboratory, Royal Fort, Tyndall Avenue,
Bristol BS8 1TL, England

(Received 28 March 1990; accepted 28 April 1990)

We report the first results of Monte Carlo simulations using hard ellipsoids with three distinct semi-axes a, b, c chosen such that $abc = 1$, $c/a = 10$ and b/a varies between 1 and 10. A survey of the phase diagram provides evidence for the existence of isotropic, nematic, discotic, and biaxial liquid crystal phases; this is believed to be the first simulation of a biaxial phase of a bulk liquid with full rotational and translational freedom. We find that the phase diagram is approximately symmetric under the transformation $\{a, b, c\} \rightarrow \{a^{-1}, b^{-1}, c^{-1}\}$, and that the biaxial phase is most stable at about the expected (self-conjugate) value $b = \sqrt{ac}$. For this value, the isotropic phase transforms directly into the biaxial phase on compression, at a density at least 50 per cent higher than that at which the nematic–isotropic transition occurs in the corresponding uniaxial systems. These results are in semi-quantitative agreement with recent theories, but there are also some significant differences.

1. Introduction

In recent years significant progress has been made in the simulation of liquid crystals using molecular models ranging from the moderately realistic to the highly idealized [1, 2]. While realistic models have remained computationally expensive it has been necessary to use simple, hard particle, models to establish the existence of orientationally ordered fluid phases of various kinds. Hard ellipsoids of revolution are known to form nematic (N_+) and discotic (N_-) phases [3]. Hard spherocylinders will form a smectic phase [4], while a cut-sphere model has been used to demonstrate columnar ordering [5].

All of these models are axially symmetric, and the removal of this restriction is an obvious next step in making the molecular model more realistic. In addition, the study of biaxial molecules leads to the possibility of simulating a bulk biaxial liquid crystal phase (B). This type of system has been studied theoretically [6–10], and the general form of the phase diagram (in shape and density variables) is expected to be as follows. For rod-like molecules a weakly first order $I \rightarrow N_+$ transition occurs on compressing the system, while for the disc-like molecules a similarly weak first order $I \rightarrow N_-$ transition is seen. However, around an intermediate crossover shape, the biaxial phase separates N_+ from N_-. The $N_+ \leftrightarrow B$ and $N_- \leftrightarrow B$ transitions are expected to be continuous, the ordering of secondary molecular axes being similar to the XY-like behaviour seen in *two dimensional* systems of highly elongated ellipses [11] and hard lines [12]. The biaxial phase extends down in density to meet the isotropic phase. All four lines of transition meet at a bicritical point, the weak $N_\pm \rightarrow I$ transitions weakening further and actually becoming continuous at this point. Detailed theoretical studies of the phase diagram have been carried out for hard spheroplatelets and hard ellipsoids [9, 10].

0267-8292/90 $3.00 © 1990 Taylor & Francis Ltd

In either case, taking a, b and c to measure the length, breadth and width respectively of the hard body concerned, the crossover shape is predicted to be for b equal to, or slightly above, the value $b = \sqrt{(ac)}$. In the simplest approximations [6–8] a symmetry relation exists under the transformation $\{a, b, c\} \leftrightarrow \{a', b', c'\} \equiv \{c, ac/b, a\}$, and this leads to the identification of $b = \sqrt{(ac)}$ as a self-dual point. More specifically, as set out by Mulder [9], Straley's theory expresses the two body interaction parameters as linear combinations of terms involving coefficients $abc, a(b^2 + c^2)$ and cyclic permutations thereof. If we compare systems of molecules of equal volume, i.e. we set $abc = a'b'c' = 1$ for convenience, then this transformation is simply $\{a, b, c\} \leftrightarrow \{a', b', c'\} \equiv \{a^{-1}, b^{-1}, c^{-1}\}$, under which all of these coefficients are invariant. In the uniaxial limit ($a = b \neq c$ for example) this transformation is the well-known rod ↔ disc interconversion, which is reflected in the approximate symmetry of the phase diagram of hard ellipsoids of revolution [3] and the exact equality of reduced second virial coefficients for conjugate pairs of these molecules.

The more recent theoretical treatments of biaxial systems [9, 10] attempt to discuss the limitations of this approximate prediction, and to calculate the density at which the bicritical point is to be found. However, to date, no simulation evidence to test the theories has been forthcoming. In this paper we describe the first steps in this direction: the Monte Carlo simulation of a system of ellipsoids with $c/a = 10$ and b/a in the range $1 \leqslant b/a \leqslant 10$, and for densities covering the full fluid range. In the uniaxial limits $b/a = 1$ and $b/a = 10$ this system is known to have well-defined $N_{\pm} \leftrightarrow I$ transitions at about 25 percent of the close-packed density, well below any solid–fluid freezing transition. Thus, we expect to see the way in which increasing molecular biaxiality influences these transitions, and to be able to see a biaxial liquid crystal over a reasonable range of densities around the crossover shape $b/a = \sqrt{10}$.

Because of the nature of the phase transitions in these systems, and the requirement to simulate large systems of quite anisometric molecules, we expect to have difficulty in locating the transitions and the bicritical point with any degree of accuracy. Very sluggish behaviour, giving rise to metastable states, will occur. None the less this first survey will point the way to more extensive simulations to follow. Here we attempt to answer two questions; does the phase diagram have the expected general form?, and approximately what is the extent of the biaxial phase?

2. Simulation details

We studied a system of $N = 343$ molecules in truncated octahedral periodic boundary conditions; normal Metropolis Monte Carlo techniques were used [13, 14]. At each move for each molecule a combined random translation and rotation was attempted. A check for overlaps with neighbouring molecules was made, and the move accepted if no overlaps were detected. It proved convenient to represent the molecular orientations using quaternion parameters, and to rotate the molecules using Vesely's prescription [15]. The sizes of rotational and translational moves were adjusted to give an acceptance rate of 40–50 per cent.

The Perram–Wertheim overlap criterion [16] was employed. This is expressed in terms of a function $F^{\mathrm{PW}}(\mathbf{\Omega}_i, \mathbf{\Omega}_j, \mathbf{r}_{ij})$ of the orientations $\mathbf{\Omega}_i, \mathbf{\Omega}_j$ and centre-to-centre vector $\mathbf{r}_{ij}$ of each pair of molecules. The value $F^{\mathrm{PW}} = 1$ corresponds to a pair in contact, overlapping pairs having $F^{\mathrm{PW}} < 1$ and non-overlapping pairs $F^{\mathrm{PW}} > 1$. F^{PW} is evaluated by numerical maximization of a function $F(\lambda)$

$$F^{\mathrm{PW}} = \max_{0 \leqslant \lambda \leqslant 1} F(\lambda), \tag{1}$$

but non-overlapping pairs are often quickly detected in a simulation by finding $F(\lambda) > 1$ for $\lambda = \frac{1}{2}$.

The pressure was calculated using the method of Vieillard-Baron [17] as formulated by Perram *et al.* using their overlap function [16]. For these systems this method is precisely equivalent to that of Eppenga and Frenkel [18]: it amounts to counting the number of pair overlaps which would result from a very small uniform scaling of the particle size (or system density). Specifically we write

$$Z \equiv \frac{PV}{NkT} - 1 = \frac{2\langle N_{\text{overlap}} \rangle}{3N\varepsilon}, \tag{2}$$

where $\langle \dots \rangle$ is a simulation average, and N_{overlap} is the number of pair overlaps which would result in the N molecule system from applying the modified overlap criterion $F^{\text{PW}} < 1 + \varepsilon$, ε being a specified small number. This corresponds to scaling all particle dimensions by a factor $(1 + \varepsilon)^{1/2}$, or alternatively the system density by a factor $(1 + \varepsilon)^{3/2}$, i.e. $\Delta\rho/\rho = \frac{3}{2}\varepsilon$. We followed Perram *et al.* [16] in using a value of $\varepsilon = 0{\cdot}01$, which proved to be satisfactory.

Four second rank order parameters characterize uniaxial and biaxial ordering in these systems [8, 9]

$$\left.\begin{aligned} Q^2_{00} &\equiv \langle \tfrac{1}{2}(3\cos^2\theta - 1)\rangle, \\ Q^2_{20} &\equiv \langle \tfrac{1}{2}\sqrt{3}\sin^2\theta\cos 2\phi\rangle, \\ Q^2_{20} &\equiv \langle \tfrac{1}{2}\sqrt{3}\sin^2\theta\cos 2\psi\rangle, \\ Q^2_{22} &\equiv \langle \tfrac{1}{2}(1 + \cos^2\theta)\cos 2\phi\cos 2\psi - \cos\theta\sin 2\phi\sin 2\psi\rangle, \end{aligned}\right\} \tag{3}$$

where θ, ϕ and ψ are the Euler angles of a typical molecule with respect to the laboratory axes. In practice only two of these parameters, Q^2_{00} and Q^2_{22} are significant, the former being the usual uniaxial order parameter measuring the alignment of the principal molecular axis (z) with the director (taken to be in the Z direction), and the latter being sensitive to the alignment of the subsidiary (x and y) molecular axes along the laboratory X and Y directions. This can be seen more easily if we re-write the definitions in cartesian form. Define a dyadic formed from the unit vectors $\hat{\mathbf{x}}_i$, $\hat{\mathbf{y}}_i$, $\hat{\mathbf{z}}_i$, along each of the axes of molecule i, summed over all molecules:

$$Q^{xx}_{\alpha\beta} \equiv \frac{1}{N}\sum_{i=1}^{n} (\tfrac{3}{2}\hat{x}_{i\alpha}\hat{x}_{i\beta} - \tfrac{1}{2}\delta_{\alpha\beta}), \quad \alpha, \beta = 1, 2, 3, \tag{4}$$

with similar definitions for $Q^{yy}_{\alpha\beta}$ and $Q^{zz}_{\alpha\beta}$; $\delta_{\alpha\beta}$ is the Kronecker delta. Then the order parameters are

$$\left.\begin{aligned} Q^2_{00} &\equiv \langle \mathbf{Z}\cdot\mathbf{Q}^{zz}\cdot\mathbf{Z}\rangle, \\ Q^2_{22} &\equiv \tfrac{1}{3}\langle \mathbf{X}\cdot\mathbf{Q}^{xx}\cdot\mathbf{X} + \mathbf{Y}\cdot\mathbf{Q}^{yy}\cdot\mathbf{Y} - \mathbf{X}\cdot\mathbf{Q}^{yy}\cdot\mathbf{X} - \mathbf{Y}\cdot\mathbf{Q}^{xx}\cdot\mathbf{Y}\rangle. \end{aligned}\right\} \tag{5}$$

Apart from finite-size corrections, Q^2_{00} should be zero in an isotropic phase, and will be non-zero, increasing towards its maximum value of 1, in a uniaxial (or biaxial) phase. Similarly, Q^2_{22} should be zero in an isotropic or uniaxial phase, and will be non-zero, increasing towards its maximum value of 1, in a biaxial phase.

In the simulation the principal and subsidiary molecular axes must be identified, of course, and the laboratory X, Y and Z directions are also to be determined. An unambiguous procedure for this was developed, based solely on the assumption that the appropriate molecular axes could be identified with the axes of symmetry of the molecule rather than being arbitrarily oriented in the molecule. First, for each of the molecular symmetry axes, these dyadics were calculated. In each case the set of three eigenvalues and eigenvectors were determined, the top eigenvalue λ_+ and its corresponding eigenvector being of interest. The molecular axis corresponding to the largest λ_+ was then identified as the principal molecular axis z, the corresponding eigenvector was identified as the laboratory Z direction, and the eigenvalue was equal to $\mathbf{Z} \cdot \mathbf{Q}^{zz} \cdot \mathbf{Z}$. This is the usual procedure for calculating the nematic order parameter [19] the only complication being the need to decide amongst the three possible molecular axes. The second largest λ_+ was taken to identify the secondary molecular ordering axis y. The corresponding eigenvector was used to construct the second laboratory axis Y, it being only necessary to orthogonalize with respect to Z. The remaining molecular axis was taken to be x, while X was constructed perpendicular to Y and Z. With these axes defined, the instantaneous order parameters were straightforwardly calculated from equation (5) ready for averaging over the simulation run.

A range of molecular shapes with semiaxes a, b, c was examined. For a fixed ratio $c/a = 10$, the following values of b/a were studied over the full liquid density range: $b/a = 2{\cdot}0, 2{\cdot}5, 2{\cdot}818, 3{\cdot}162, 3{\cdot}548, 4{\cdot}0, 5{\cdot}0$. These values were chosen to lie at convenient intervals on a logarithmic scale of b/a. The value $b/a = 3{\cdot}162 = \sqrt{10}$ is the expected approximate crossover shape, and the pairs $(2{\cdot}0, 5{\cdot}0)$, $(2{\cdot}5, 4{\cdot}0)$ and $(2{\cdot}818, 3{\cdot}548)$ are conjugate shapes in the sense of the previous section. Results for $b/a = 1$ and $b/a = 10$ have been obtained previously using a larger system size of $N = 500$ [1] and employing the molecular dynamics method. Densities in the range $0{\cdot}2 \leqslant \rho/\rho_{\mathrm{cp}} \leqslant 0{\cdot}6$ were studied for every shape. Here ρ_{cp} is the close packing density which is given by $8\rho_{\mathrm{cp}}abc = \sqrt{2}$ assuming that the structure is obtained by scaling a close packed hard sphere crystal by factors of a, b and c in three perpendicular directions. The hard sphere system freezes at $\rho/\rho_{\mathrm{cp}} \approx 0{\cdot}67$, and slightly higher transition densities are seen for those ellipsoids of revolution studied thus far [3], so the chosen densities are all expected to lie within the fluid range. In addition, more extreme shapes $b/a = 1{\cdot}259$, $1{\cdot}585$, $6{\cdot}310$, $7{\cdot}943$ were studied at $\rho/\rho_{\mathrm{cp}} = 0{\cdot}4, 0{\cdot}5$, to confirm further the smooth extrapolation of the results reported here to those obtained earlier for $b/a = 1, 10$.

Several sequences of runs were carried out. A typical run would start from the final configuration of a simulation at a nearby density or molecular shape. At each state point an equilibration period of about 10^4 Monte Carlo sweeps (moves per particle) was allowed, and then a production run of at least a further 10^4 sweeps was carried out. Close to the phase transitions runs of up to five times this length were employed. We adjusted densities and shapes in both directions, checking for hysteresis and discrepancies in the results. Most of the results reported here are for sequences starting originally from an orientationally ordered, perfect biaxial, configuration, and then progressively changing the density from one state point to the next. However, checks in the reverse direction were also carried out as we now describe.

The starting point was prepared as follows. For five of the shapes, $b/a = 2{\cdot}0, 2{\cdot}5, 3{\cdot}162, 4{\cdot}0, 5{\cdot}0$, an oriented fluid at $\rho/\rho_{\mathrm{cp}} = 0{\cdot}5$ was obtained by slow uniform compression of a dilute system, allowing Monte Carlo translational moves, but keeping perfect orientational alignment. Having achieved the desired reduced density the orientational constraint was removed, and the system allowed to equilibrate. Some systems remained biaxial, others quickly converted to uniaxial nematic or discotic phases. In each case, following equilibration, production runs were carried out. The density was then progressively changed up or down, additional time allowed for equilibration at each new state point, and results accumulated at the new density. As the density was lowered, a transition to the isotropic liquid was seen at some point, for each shape.

Having carried out these sequences, additional runs were conducted by uniform compression from the disordered isotropic phase, to observe the spontaneous formation of orientationally ordered states. In addition, the two near-crossover shapes $b/a = 2{\cdot}818, 3{\cdot}548$ were studied at densities $\rho/\rho_{\text{cp}} = 0{\cdot}5, 0{\cdot}6$ by equilibrating at constant density, but converting the shape from a previously equilibrated nearby state point. Approaches were made from both the $b/a = 3{\cdot}162$ shape (biaxial phase) and from $b/a = 2{\cdot}5, 4$ respectively (both in the uniaxial phase).

3. Results

The excess pressures $Z = PV/NkT - 1$ and orientational order parameters obtained from these simulation runs are given in tables 1 and 2. We estimate the statistical errors on Z to be of order 5 per cent, and on the order parameters to be of order 10 per cent, but the systematic errors due to poor equilibration near the phase transitions may be much more serious, as we have discussed. Hence these results should be treated with some caution, and we bear this in mind later.

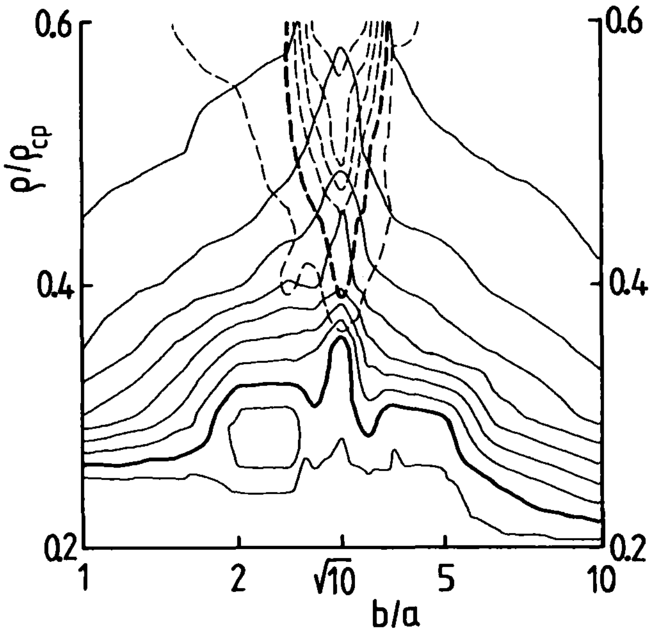

Figure 1. Contours of the orientational order parameters Q^2_{00} (solid lines) and Q^2_{22} (dashed lines) in the shape-density plane. Density is expressed as ρ/ρ_{cp} where ρ_{cp} is the close packed density, and the axial ratio b/a is represented on a logarithmic scale. The contour interval is 0·1 and the contour at 0·2 is highlighted in each case.

The principal result of this paper is the rough determination of the phase diagram as revealed by calculating the uniaxial and biaxial order parameters Q^2_{00} and Q^2_{22}. In figure 1 we show contours of Q^2_{00} and Q^2_{22} on the shape-density phase diagram. These results are obtained from the sequences of runs originating in the orientationally ordered phases (see table 1). It is quite possible that much longer runs would reveal some of the ordered phase state points close to the transition to be metastable,

Table 1. Results for simulation sequences which progress from more ordered to less ordered phases.

ρ/ρ_{cp}	Q^2_{00}	Q^2_{22}	Z	Q^2_{00}	Q^2_{22}	Z
		$b/a = \sqrt{10}$				
0·20	0·06	0·03	2·69			
0·25	0·06	0·03	3·70			
0·30	0·12	0·06	4·78			
0·35	0·11	0·04	5·97			
0·40	0·52	0·24	6·65			
0·45	0·57	0·28	7·78			
0·50	0·75	0·56	8·47			
0·55	0·77	0·58	10·24			
0·60	0·82	0·71	12·25			
		$b/a = 2{\cdot}818$			$b/a = 3{\cdot}548$	
0·20	0·06	0·04	2·68	0·07	0·04	2·72
0·30	0·18	0·08	4·65	0·25	0·05	4·68
0·40	0·62	0·07	6·39	0·67	0·10	6·22
0·50	0·78	0·34	8·77	0·81	0·28	8·70
0·60	0·86	0·63	12·31	0·86	0·61	12·37
		$b/a = 2{\cdot}5$			$b/a = 4$	
0·20	0·06	0·03	2·64	0·05	0·04	2·79
0·25	0·11	0·04	3·66	0·08	0·03	3·83
0·30	0·06	0·06	4·80	0·12	0·05	4·81
0·35	0·34	0·04	5·84	0·55	0·03	5·40
0·40	0·59	0·11	6·41	0·70	0·06	6·25
0·45	0·76	0·09	7·13	0·80	0·09	7·06
0·50	0·83	0·15	8·61	0·87	0·04	8·28
0·55	0·88	0·19	10·30	0·89	0·07	10·12
0·60	0·92	0·18	12·48	0·91	0·12	12·70
		$b/a = 2$			$b/a = 5$	
0·20	0·05	0·04	2·68	0·06	0·03	2·84
0·25	0·11	0·04	3·67	0·08	0·03	3·87
0·30	0·07	0·03	4·88	0·20	0·04	4·74
0·35	0·36	0·04	5·82	0·65	0·07	4·95
0·40	0·72	0·04	6·04	0·75	0·04	5·72
0·45	0·82	0·07	6·66	0·83	0·05	6·69
0·50	0·87	0·06	7·99	0·89	0·05	7·81
0·55	0·90	0·10	9·64	0·92	0·09	9·65
0·60	0·93	0·15	11·82	0·93	0·08	11·80
		$b/a = 1{\cdot}585$			$b/a = 6{\cdot}310$	
0·40	0·78	0·06	5·64	0·82	0·03	5·38
0·50	0·90	0·04	7·53	0·91	0·06	7·43
		$b/a = 1{\cdot}259$			$b/a = 7{\cdot}943$	
0·40	0·82	0·05	5·45	0·86	0·04	5·29
0·50	–	–	–	0·92	0·04	7·35

Table 2. Results for simulation sequences which progress from less ordered to more ordered phases.

ρ/ρ_{cp}	Q^2_{00}	Q^2_{22}	Z	Q^2_{00}	Q^2_{22}	Z
		$b/a = \sqrt{10}$				
0·40	0·23	0·09	7·18			
0·45	0·49	0·13	8·32			
0·50	0·66	0·33	9·23			
		$b/a = 2·818$			$b/a = 3·548$	
0·50	0·79	0·18	8·86	0·82	0·16	8·70
0·60	0·89	0·27	12·72	0·90	0·13	12·70
		$b/a = 2·5$			$b/a = 4$	
0·35	0·21	0·05	5·96	0·25	0·05	5·80
0·40	0·38	0·08	6·95	0·32	0·11	6·76
0·45	0·61	0·16	7·86	0·60	0·17	7·49
0·50	0·73	0·21	9·03	0·78	0·08	8·60
		$b/a = 2$			$b/a = 5$	
0·30	-	-	-	0·17	0·04	4·84
0·35	0·14	0·02	6·20	0·31	0·06	5·67
0·40	0·34	0·04	7·06	0·55	0·08	6·22
0·45	0·60	0·05	7·55	0·84	0·06	6·63
0·50	0·79	0·12	8·50	0·89	0·08	7·87

not thermodynamically stable, and this would displace some of the contours upwards in density. The contours are plotted at intervals of 0·1, and we have highlighted the contour value $Q = 0·2$ in each case to give a guide to the location of the phase transition lines, but alternative choices are possible. Because of the way we have calculated the order parameters, they are both guaranteed to be positive and of order $\mathcal{O}[\sqrt{(1/N)}] \approx 0·05$ even in the isotropic phase, and they will have statistical fluctuations of similar size superimposed on them. The exact shape of the lowest contour $Q = 0·1$ in each case is therefore not very significant. Since we have chosen density rather than pressure to specify the state point in this diagram, we expect there to be coexistence regions for the first order $\mathrm{N}_\pm \leftrightarrow \mathrm{I}$ phase transitions, but these transitions are so weak that the coexisting densities will be quite close and we make no attempt to distinguish them on the basis of these results.

The shape parameter b/a is plotted on a logarithmic scale, and with this choice the phase diagram is approximately symmetric about the self-conjugate crossover shape. However, unsymmetrical features are apparent. The uniaxial order parameter contours are shifted to slightly lower densities for the disc-like spheroids compared with their rod-like counterparts, in agreement with previous results for the extreme cases $b/a = 1, 10$ [1] and for other axially symmetric systems [3].

The biaxial region seems to be restricted to a rather narrow range of shapes. If we ignore the behaviour of the $Q^2_{22} = 0·1$ contour as being insignificant, we cannot claim to see any displacement of the biaxial region in either direction from the self-conjugate value $b/a = \sqrt{10}$, nor much evidence of asymmetry about this line in the diagram. Our results provide only a crude guide to the location of the $\mathrm{B} \leftrightarrow \mathrm{N}_\pm$ transition lines, which are quite steep.

As a first attempt to assess the problem of metastability, we compare in figure 2 the results from the expansion runs with those from the compression runs started from the isotropic limit. It is clear that there are some problems in the vicinity of the I → $N_{\pm}$/B transitions, and that further work is needed to locate these transition densities accurately. None the less it is also clear that the appropriate ordered phases *are* formed spontaneously on compression. In particular at the crossover shape the isotropic phase is converted directly into a biaxial phase, although hysteresis/ metastability is seen in both Q^2_{00} and Q^2_{22}; the biaxial order parameter seems to be the more sluggish in response to compression on this simulation time scale.

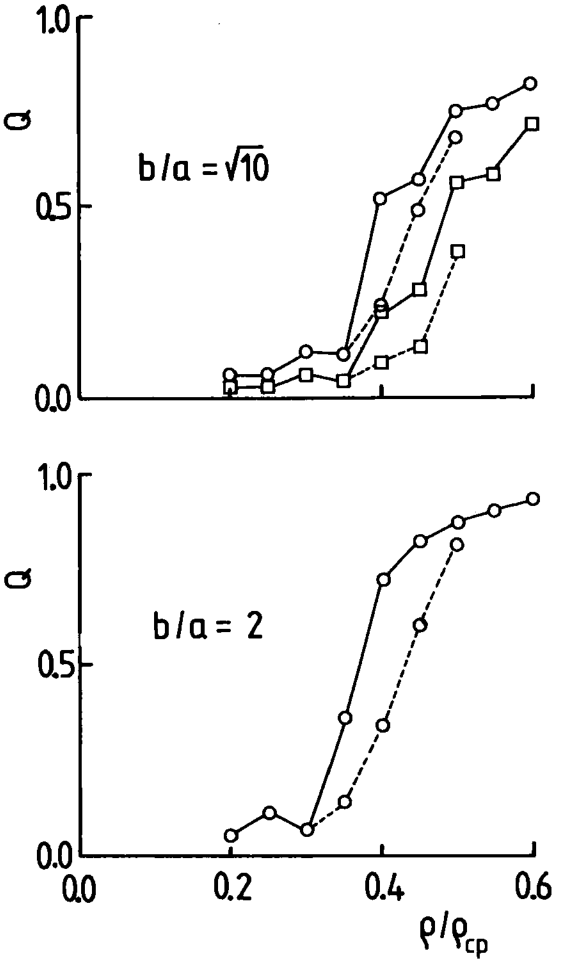

Figure 2. Order parameters as functions of density for two shapes $b/a = \sqrt{10}, 2$. We show the uniaxial parameter Q^2_{00} (circles) for both shapes and the biaxial parameter Q^2_{22} (squares) for $b/a = \sqrt{10}$. Solid lines join results of sequences of runs progressing from high to low density. Dashed lines join results of sequences progressing from low to high density.

To follow up this point, we present in figure 3 the time evolution (in the Monte Carlo sense) of the order parameters as seen on compressing the $b/a = \sqrt{10}$ system. It is clear that proper equilibrium has not been attained for the $\rho/\rho_{cp} = 0{\cdot}45$ system, but that both order parameters are continuing to increase, and that this is also true for $\rho/\rho_{cp} = 0{\cdot}50$ even after more than 35 000 sweeps. None the less, there are indications that the biaxial phase is forming at $\rho/\rho_{cp} = 0{\cdot}45$, and it is clearly stable at $\rho/\rho_{cp} = 0{\cdot}50$; much longer runs should give reliable agreement between expanding and compressing sequences.

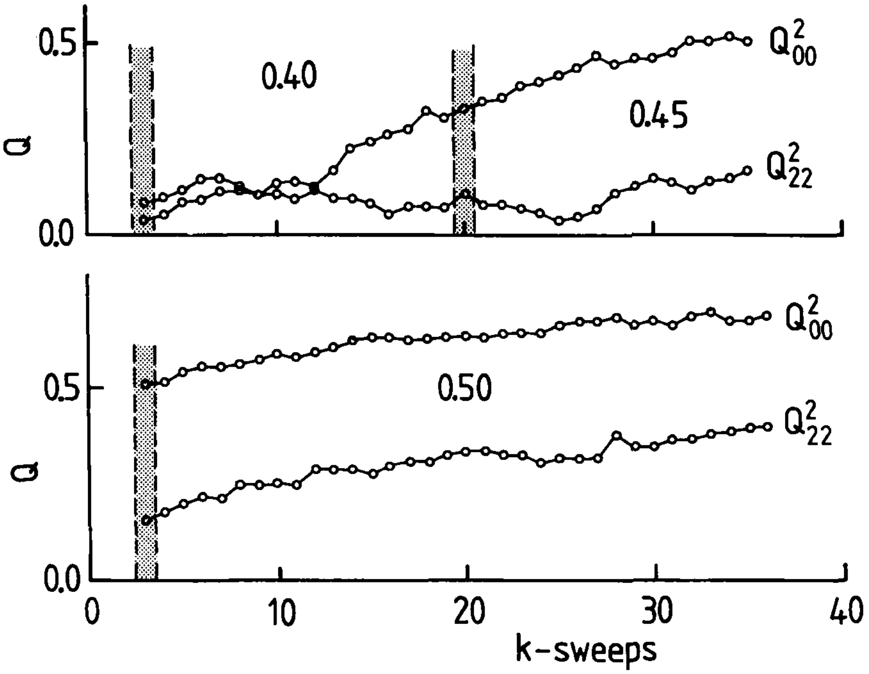

Figure 3. Uniaxial (Q^2_{00}) and biaxial (Q^2_{22}) order parameters as function of Monte Carlo time (in sweeps, i.e. attempted moves per particle) for compression of the $b/a = \sqrt{10}$ system. The densities $\rho/\rho_{cp} = 0{\cdot}40, 0{\cdot}45, 0.50$ are indicated. The shaded regions denote periods of 1000 sweeps during which the density was uniformly changed from one value to the next.

These general features are echoed in the behaviour of the pressure, as measured by $Z = PV/NkT - 1$. We compare, in figure 4 Z as a function of density for the crossover shape $b/a = \sqrt{10}$ with the results for the rod-like molecules. A similar comparison with the disc-like molecules is made in figure 5. Once again we highlight the metastability problem. It should be emphasized that the results for $b/a = 1, 10$, included here for comparison, were obtained using much longer simulation runs, and employing molecular dynamics rather than Monte Carlo. They do not suffer from such extensive metastability, although in the immediate vicinity of the phase transition (where Z apparently drops as ρ increases, while the system changes from one branch of the equation of state to the other) there is an effect. One additional point of interest emerges from these figures. For both rod-like and disc-like shapes, the equation of state curve seems to vary less dramatically at the transition as the molecules lose their axial symmetry. This may be consistent with the expected weakening of the transition, but more direct evidence is required to confirm this.

Finally, in figure 6 we plot Z as a function of shape for each of the reduced densities. Within the isotropic and nematic phases we can see that our results extrapolate smoothly over to the uniaxial $b/a = 1, 10$ limits. There is a surprising apparent discontinuity in the curves on crossing the tentative $\mathrm{B} \leftrightarrow \mathrm{N}_{\pm}$ phase boundaries. Note that almost all of our biaxial phase simulations are for the cross-over shape $b/a = \sqrt{10}$. On the basis of the simulation runs conducted for $b/a = 2{\cdot}818, 3{\cdot}548$ we believe that these shapes lie just within the biaxial region for $\rho/\rho_{\mathrm{cp}} = 0{\cdot}6$, but outside it for $\rho/\rho_{\mathrm{cp}} = 0{\cdot}5$. The overall imperfect symmetry of the equation of state with respect to conjugate molecular shapes is again evident.

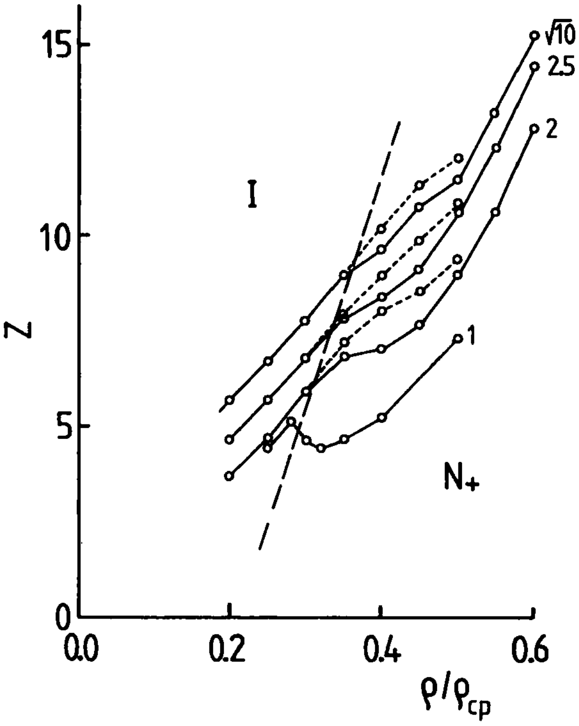

Figure 4. $Z = PV/NkT - 1$ versus reduced density for $b/a = \sqrt{10}$ compared with results for rod-like molecules. Solid lines join results of sequences of runs progressing from high to low density. Dashed lines join results of sequences progressing from low to high density. The long dashes divide state points identified as belonging to the isotropic phase (I) from those belonging to the nematic phase (N_+).

4. Discussion and conclusions

Our simulation results are clearly very crude first estimates, in the vicinity of the phase transitions, for the reasons set out in the introduction. In the case of hard ellipsoids of revolution, the transition densities for the weakly first-order N → I transition could be estimated [3] by free energy calculation. It has been suggested [20] that even a small amount of molecular biaxiality may dramatically further weaken this transition, thus making it much more difficult to locate the intersection point of free energy curves. Our simulations seem to be consistent with the weakening of the transition, but additional work is necessary before quantitative conclusions can be drawn. As the biaxiality increases we may expect pretransitional fluctuations, already observed for the axially symmetric case [21] to be more dominant. The $\mathrm{B} \leftrightarrow \mathrm{N}_{\pm}$ transition is expected to be continuous, *XY* like, with long ranged algebraic decay of correlations; to characterize it will probably require larger system sizes and longer

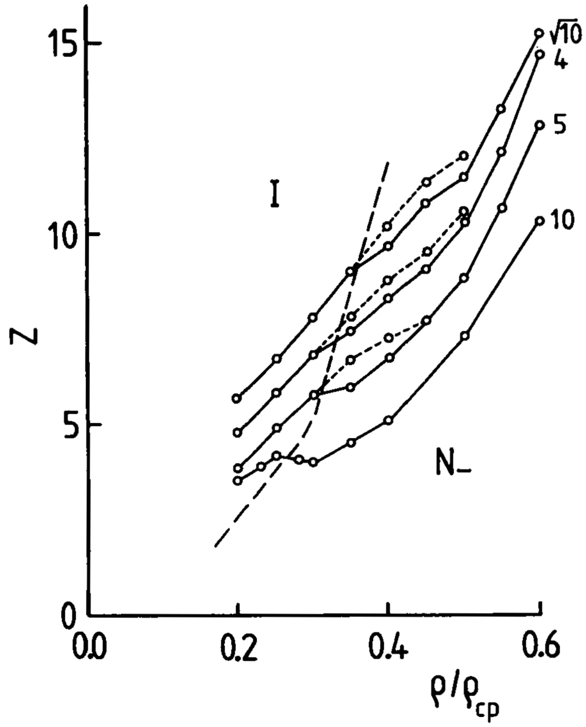

Figure 5. $Z = PV/NkT - 1$ versus reduced density for $b/a = \sqrt{10}$ compared with results for disc-like molecules; notation as for figure 4. The long dashes divide state points identified as belonging to the isotropic phase (I) from those belonging to the discotic phase (N_-).

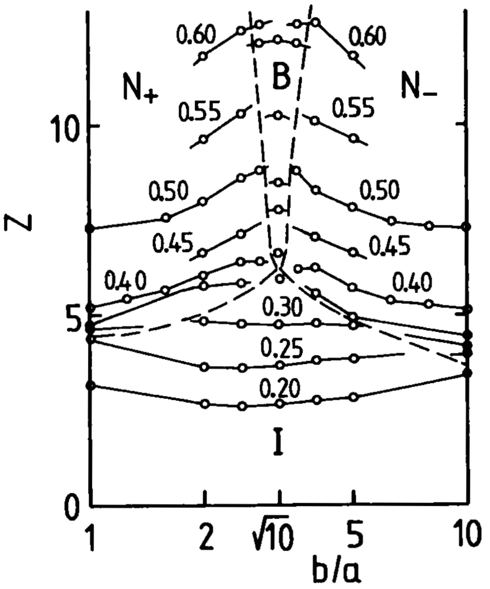

Figure 6. $Z = PV/NkT - 1$ versus b/a (solid lines) for various reduced densities ρ/ρ_{cp}. b/a is represented on a logarithmic scale. The dashed lines separate state points identified as belonging to different phases, and we break the solid lines where they cross these.

simulation times than were available for this study. Our simulation results certainly show evidence of insufficient simulation times around the phase transitions.

None the less, with these caveats in mind, the approximate phase diagram determined here is likely to be a reasonable guide. The general form is indeed as expected, with a biaxial phase separating nematic and discotic uniaxial phases. The transition from isotropic to orientationally ordered liquid is displaced up in density at about the crossover shape $b \approx \surd(ac)$, relative to its position for more rod-like or disc-like shapes, because of the presence of the biaxial phase above. Close to this shape the system presumably postpones the transition because, on forming the ordered phase, it must sacrifice most of its orientational disorder at once. Away from this shape the system can give up just part of its orientational disorder, forming a uniaxial phase, as a trade for greater overall freedom, and it does this more readily. Our estimates of the transition densities are likely to be *lower* bounds, because the metastability effects will have overestimated the range of the ordered phase. Consequently we can say the the bicritical point occurs at a density $\rho/\rho_{cp} \approx 0{\cdot}4$ or greater, at least 50 per cent higher than the reference N ↔ I transition in the corresponding uniaxial systems. The bicritical point seems to be quite close to the shape $b = \surd(ac)$, but our results are not sufficiently accurate or reliable to suggest whether it in fact lies to one side or the other of this value. In the ordered phase, the biaxial region seems to cover a quite narrow range of molecular shapes (and here again, because of metastability, we have essentially established an *upper* bound on the range of this phase) right up to the highest densities where we expect the solid phase to appear. Clearly much more effort must be concentrated in the region $2{\cdot}5 < b/a < 4$ before we can draw more definite conclusions regarding the biaxial phase.

We can attempt to compare our preliminary results with the smoothed density approximation of Hołyst and Poniewierski [10] for the location of the bicritical point. Unfortunately they were only able to study the hard ellipsoid system for $c/a \leqslant 7$, so we must extrapolate their results to $c/a = 10$. They predict that the bicritical shape ratio $b/\surd(ac)$ deviates slightly from unity as c/a increases. The difference $b/\surd(ac) - 1$ is small (a few per cent) but quite strongly varying. A plot of $\log(b/\surd(ac) - 1)$ versus $\log(c/a)$ is moderately linear, and an extrapolation to $c/a = 10$ gives $b/\surd(ac) \approx 1{\cdot}2$, i.e. a shift of 20 per cent from $b/a = \surd 10$ to almost 4. Our results certainly do not seem to be consistent with such a large shift, but of course the extrapolation of the theoretical predictions may not be trustworthy. Better agreement is seen with the predicted bicritical density, which decreases steadily as c/a increases. We estimate an extrapolated value of $\rho/\rho_{cp} \approx 0{\cdot}35$–$0{\cdot}40$, which agrees well with our simulation results.

Further simulation work should now concentrate on examining the free energies in the vicinity of the $N_\pm \leftrightarrow I$ transitions, and on determining their order, as well as locating more accurately the $B \leftrightarrow N_\pm$ transition lines and studying the range of spatial correlations in the ordered phases. This work is currently in progress.

The simulations reported here were carried out on the Bristol University IBM 3090-150 VF; thanks are due to the Computer Centre Staff for advice and assistance. Conversations with D. Frenkel and B. Mulder, and support for international travel from NATO, are also gratefully acknowledged.

References

[1] ALLEN, M. P., and WILSON, M. R., 1989, *J. Comput. Aided Molec. Design*, **3**, 335.

[2] FRENKEL, D., 1987, *Molec. Phys.*, **60**, 1.

[3] FRENKEL, D., MULDER, B. M., and MCTAGUE, J. P., 1984, *Phys. Rev. Lett.*, **52**, 287. FRENKEL, D., and MULDER, B. M., 1985, *Molec. Phys.*, **55**, 1171.

[4] FRENKEL, D., LEKKERKERKER, H. N. W., and STROOBANTS, A., 1988, *Nature, Lond.*, **332**, 822.

[5] FRENKEL, D., 1989, *Liq. Crystals*, **5**, 929.

[6] FREISER, M. J., 1970, *Phys. Rev. Lett.*, **24**, 1041. For a Monte Carlo simulation of this type of lattice model see LUCKHURST, G. R., and ROMANO, S., 1980, *Molec. Phys.*, **40**, 129.

[7] ALBEN, R., 1973, *Phys. Rev. Lett.*, **30**, 778.

[8] STRALEY, J. P., 1974, *Phys. Rev.* A, **10**, 1881.

[9] MULDER, B. M., 1986, *Liq. Crystals*, **1**, 539; 1989, *Phys. Rev.* A, **39**, 360.

[10] HOLYST, R., and PONIEWIERSKI, A., 1990, *Molec. Phys.*, **69**, 193.

[11] CUESTA, J. A., and FRENKEL, D., *Phys. Rev.* A (to be published).

[12] FRENKEL, D., and EPPENGA, R., 1985, *Phys. Rev.* A, **31**, 1776.

[13] METROPOLIS, N., ROSENBLUTH, A. W., ROSENBLUTH, M. N., TELLER, A. H., and TELLER, E., 1953, *J. chem. Phys.*, **21**, 1087.

[14] ALLEN, M. P., AND TILDESLEY, D. J., 1987, *Computer Simulation of Liquids* (Clarendon).

[15] VESELY, F. J., 1982, *J. Comput. Phys.*, **47**, 291.

[16] PERRAM, J. W., WERTHEIM, M. S., LEBOWITZ, J. L., and WILLIAMS, G. O., 1984, *Chem. Phys. Lett.*, **105**, 277. PERRAM, J. W., and WERTHEIM, M. S., 1985, *J. comput. Phys.*, **58**, 409.

[17] VIEILLARD-BARON, J., 1972, *J. chem. Phys.*, **56**, 4729.

[18] EPPENGA, R., and FRENKEL, D., 1984, *Molec. Phys.*, **52**, 1303.

[19] ZANNONI, C., 1979, *The Molecular Physics of Liquid Crystals*, edited by G. R. Luckhurst and G. W. Gray (Academic Press), Chap 3.

[20] GELBART, W. M., and BARBOY, B., 1980, *Accts chem. Res.*, **13**, 290.

[21] ALLEN, M. P., and FRENKEL, D., 1987, *Phys. Rev. Lett.*, **58**, 1748.